AD-A075 284 VIRGINIA POLYTECHNIC INST AND STATE UNIV BLACKSBURG --ETC F/G 14/2
NONDESTRUCTIVE EVALUATION OF DAMAGE IN METAL MATRIX COMPOSITES.(U)
JAN 79 E G HENNEKE, K L REIFSNIDER N00014-78-C-0153

UNCLASSIFIED NL

| OF |
AD A
075284

END
DATE FILMED
11 -79
DDC

(12)

(6) # NONDESTRUCTIVE EVALUATION OF DAMAGE IN METAL MATRIX COMPOSITES

by

(10) Edmund G. Henneke, Kenneth L. Reifsnider
Wayne W. Stinchcomb and John C. Duke
Department of Engineering Science and Mechanics
Virginia Polytechnic Institute and State University
Blacksburg, Virginia 24061

(15) Interim Technical Report
for Contract No. N00014-78-C-0153

(11) 31 January 1979

(12) 53

(9) Interim technical rept.,

TABLE OF CONTENTS

1.0 Report Summary

The major purpose of the present work was to develop a technical base for the application of nondestructive evaluation methods to metal matrix composites. To fulfil this aim, several objectives were established: (1) To obtain base line data on non-destructive evaluation methods applied to metal matrix, fiber-reinforced composite coupon specimens with controlled, fabricated flaws; (2) To investigate ways of modifying NDE methods for application to specimens having geometries other than the flat coupon specimens; and (3) To apply appropriate NDE methods to other specimens that would be mechanically tested elsewhere. In particular, these NDE methods should provide quantitative parameters that could be correlated with the mechanical properties.

During the first year of the project, effort has been spent in obtaining Al/Fp and Al/W composite specimens having both flat coupon and circular cylinder geometries. In the case of Al/Fp, because of fabrication procedures, it was impossible for the supplier to provide specimens with controlled flaws. Once obtained, the Al/Fp specimens have been used in the laboratory to obtain preliminary information on the ability of several different NDE methods to interrogate fiber-reinforced metal matrix composites. The methods considered to date have been ultrasonic C-scan, ultrasonic pulse-echo, eddy current, X-ray radiography, thermography and stress wave factor. In most cases, some degree of experimental development has been necessary to apply each technique to the particular specimen geometry of the composites being studied here.

The results obtained from the ultrasonic C-scan have proven to be most interesting to date. The C-scans indicate definite longitudinal

layers parallel to the long axis of the Al/Fp specimens. It is believed that these layers are indicative either of the original layers of material that were used in laying up the panel from which the specimens were cut or of the flow paths of the molten matrix material as it filled the mold during fabrication. The 12.7 mm (1/2 in) wide specimens were cut from a 12.7 mm (1/2 in) thick panel and hence the flats, or widths, of the specimens studied here were perpendicular to the laminae formed by the prepreg tape used in constructing the panel. In any case, in the coming contract period, these specimens will be tested in three-point bending to determine the effect, if any, of these longitudinal striations on the mechanical properties.

In support of this project, Virginia Polytechnic Institute and State University has purchased a Faxitron X-ray radiographic unit using in-house funds. This unit is capable of producing soft (low energy) X-rays that can be used to radiograph composite materials such as graphite-epoxy and the metal matrix composites studied here. Preliminary work with this machine has produced radiographs that show longitudinal layering in the coupon specimens similar to those seen in the C-scans.

2.0 Experimental Techniques

2.1 Background

As discussed in the Summary section of this report, the basic objectives of this work were: to apply nondestructive evaluation techniques to metal matrix composites; to obtain base line data as to the ability of these techniques to locate, identify and quantify defects in these materials; to determine the effect of these defects on strength and stiffness; and to modify the techniques as required for application to specimens having geometries other than the flat tensile coupon. Several different nondestructive testing techniques have been considered for possible application to metal matrix composites. A description of these is given in the following pages. Some of these methods have been applied during the past year to Al/Fp fiber composites while others have been investigated in a preliminary fashion in order to determine potential problem areas that will need to be solved for proper application in the coming years.

2.2 Ultrasonic C-scan

Ultrasonic C-scans are used to obtain a qualitative plan view of regions of a specimen that, because of defects, scattering centers, or other localized material behavior, are inferior in their ability to transmit ultrasonic energy. There are several different operation modes that can be selected for obtaining C-scans of a specimen. Because of the small thicknesses of the composite plate specimens used in this work, it was found necessary to scan the specimens in such a fashion that the critical echo examined was the first echo returning from the bottom of the scanning tank, Figure 1. Specifically, in Fig. 1, the original pulse, 1, is initiated by the transducer and propagates through the water in the scanning tank. At the top surface of the specimen, a portion of the pulse, 2, is reflected and a portion, 3, is transmitted through the specimen. Neglecting further reflections that occur internally in the specimen, pulse 3 is reflected by the bottom of the tank, 4. The latter is again partially reflected, 5, and partially transmitted, 6. Pulse 6 was the echo selected for triggering the display mechanism of the C-scan recorder. A trigger level is set so that if echo 6 has an amplitude above the trigger level, the recording mechanism displays a black mark, if the echo has an amplitude below the set trigger level, the recorder pen is turned off and a white region appears.

The amplification and trigger level settings on the pulse generator are obviously very critical to obtaining a meaningful C-scan. If either the signal amplification is set too high or the trigger level is set too low, the scan will be completely black. The opposite settings will yield a scan that is totally white. Any C-scan one obtains is thus

qualitative only in that it depends upon the operator's choice of settings. C-scans can, however, be used to judge the relative quality of two specimens or the change in quality of the condition of the same specimen with load or other parameters, if appropriate experimental techniques are used to assure reproducible settings on the scanning instrumentation. Standard practice for the scanning of homogeneous materials is to use a standard, or calibration specimen, with a known flaw, quite often a flat-bottomed hole. Such a standard is not viable for the thin composite specimens that are being studied here. Considerable time was spent in selecting a standard that would yield reproducible instrumentation settings and hence reproducible C-scans. Many diverse specimens and geometries were investigated. The standard that was finally chosen has performed well in our laboratory, but is deficient in that it would be difficult to precisely duplicate for use in other laboratories.

The selected standard consists of an Al/Fp composite specimen, 12.7 x 152.4 x 2.54 mm (1/2" x 6" x 0.1,") glued to a piece of Al plate, 1.27 mm (0.050") thick, with a 6.35 mm (1/4") diameter hole (Figure 2). The ultrasonic transducer is set directly over the center of the hole in the plate and the gain settings on the pulse generator are set to obtain a particular amplitude of the first echo from the bottom of the tank travelling through the Al/Fp specimen and the hole. (An amplitude corresponding to eight divisions on the CRT was chosen.) The hole in the Al plate serves only to assure the operator that the same region of the Al/Fp specimen is always used as a transmission standard. Once the gain is set, the trigger level can be adjusted to an echo having an

amplitude corresponding to any value between 0 and 8 divisions on the CRT.

For the C-scan results that are given in Section 3.1, the trigger level refers to the selected echo height on the CRT. Runs were made on all the specimens at various trigger levels to obtain a qualitative idea of the degree of the severity of the regions in each specimen that were indicated as having inferior ultrasonic transmission properties. That is, by decreasing the trigger level, these regions will gradually become black with the worst regions being the last to disappear.

For the present experimental set-up, a focused transducer with an intermediate focal length (approximately 20 mm) and a resonant frequency of 10 MHz was used as the scanning transmitter-receiver.

2.3 X-Ray Radiography

X-ray radiography was also used to examine the Al/Fp and tungsten-aluminum specimens. Two x-ray devices were used and a third was experimented with but ultimately not used. The most successful of the two units that did produce results was a device manufactured by the Hewlett-Packard Corporation called a Faxitron. That unit, which was actually designed by the Field Emission Corporation before it was bought out by Hewlett-Packard, was intended for use in the electronics industry for the purpose of radiographing solid state circuits. Because of that, special attention was paid to resolution and definition in the design of the unit. Up to a forty-eight inch specimen-to-source distance can be used in the cabinet of the apparatus, and the x-ray source (target) has dimensions of 0.5 mm by 0.5 mm so that the geometric resolution of the unit is about 0.024 degrees. The excitation voltage can be varied from about five thousand to one hundred thirty thousand volts, giving a wide spectral range of Bremstrahlung for the purpose of resolving low-density as well as high density material details. The target material is tungsten.

Development of techniques to improve our ability to resolve detail with x-ray examination is under way. As a result of our efforts so far we (the University, with assisting funds from other contract sources) have purchased a Faxitron unit to complete the remainder of our studies. The unit should be operational by 1 February 1979. This will be a major improvement over our existing equipment, as has been shown by our investigation up to this point (see Section 3.2). X-ray examination is a natural complement to the ultrasonic techniques since it is most

sensitive to cracks, or defects, or other detail of interest that have their principal plane of definition parallel to the incident beam, i.e., perpendicular to the specimen surface. Ultrasonic methods are generally more sensitive to defects which are perpendicular to the incident beam, i.e., parallel to the specimen surface. Radiography also has the advantage of producing a visual record which facilitates interpretation of the results and the communication of information in general. So far we have shown that x-ray radiography <u>can</u> be used to resolve and record internal variations in both of the materials under investigation. Our continuing work will focus on refining the observation techniques and on interpreting our results.

2.4 Eddy Current

An Al/Fp, flat coupon specimen was investigated with eddy currents using a Nortec, NDT-3, eddy current instrument. In this instance, a straight forward application of this NDT method was performed. A pencil probe, Nortec Model 3550, 6.35 mm (1/4") diameter was used at 100 kHz to map the reactance and the resistance of the specimen along the flat side of the coupon.

2.5 Ultrasonic Pulse-Echo Method

The flat Al/Fp specimens have also been studied with the use of a modified buffer rod, ultrasonic pulse-echo method. This method utilizes a quartz buffer rod to delay the echoes sufficiently in time so that appropriate amplitude measurements can be made of the returning echoes. The technique has been described by Hayford, Henneke, and Stinchcomb [1]. Because of the higher wave speeds in Al/Fp as compared to the graphite polyimide composites previously studied in our laboratories, it was necessary to make some modifications of the technique. The difficulty is that the equipment in our laboratory is limited with respect to the minimum pulse length that can be generated. Because of the relatively large velocity in Al/Fp and the thinness of the specimens, the returning echoes overlap unless the pulse length can be made sufficiently small. In the present case a compromise had to be made in selecting an appropriate frequency and pulse length which does not completely eliminate the overlap problem. However, a consistent signal can be obtained with which relative attenutation measurements can be made to compare different regions of a specimen with one another.

This technique has the advantage of providing a quantitative parameter that can be used to correlate with such mechanical properties as failure strength [1]. It is limited, however, in that it scans an area of the specimen slightly larger than that of the transducer. For the present specimens, this means that the attenuation value obtained is an integrated value of approximately the entire width of the specimen. One can obtain, however, attenuation readings at different positions along the length of the specimen.

2.6 Video-Thermography

Video-thermography is a nondestructive technique that has proven to be quite useful in our laboratory for the study of damage in composite and homogeneous materials. Thermography is the mapping of isothermal contours on the surface of a material. Video-thermography utilizes a real-time, infrared camera - television monitoring system to obtain video representation of these contours. It has been found that the temperature profiles obtained by video-thermography are very indicative of damaged regions in the specimen.

There are basically two modes of operation that one can use to effect a temperature distribution inside a material which will distinguish areas of discontinuity or damage. The first mode, often referred to as the passive mode, requires an external heat source (e.g., a heat lamp) to heat the specimen. If different regions of the specimen have different thermal conductivities, temperature gradients will be established that can be detected by the infrared camera and presented as isothermal contours. This method requires the external heat source to uniformly heat the specimen and also requires the specimen to have an average low value of thermal conductivity. For instance, the thermal conductivity of aluminum is so high that this mode will not work in this case because the heat is conducted so rapidly through the material all gradients are quickly dispersed. The second mode of operation, the active mode, is based upon the establishment of internal heat sources that will give rise to local thermal gradients around the sources. The internal heat sources are established by the local transformation of some other form of energy into heat.

In our laboratory, the transformation of mechanical energy into

heat has been effected by two techniques. A fatigue load applied to the specimen will initiate damage in the specimen and will cause steady state heat evolution in the vicinity of the damage due to hysteresis or internal friction effects. This technique is easily applied for the real time observation of the initiation and progression of damage in the specimen. On the other hand, if one does not wish to add further damage to the material, a second technique, vibrothermography, can be used. This technique applies low amplitude, high frequency mechanical vibrations to the specimen. It has been found in our laboratory that these low amplitude vibrations are preferentially transformed to heat around certain types of damaged regions and therefore the damage is easily detected by video-thermography. It should be emphasized that the vibrations induced in the specimens give rise to extremely small strains and hence it is very unlikely that any additional damage is added to the specimen by this technique.

Thermography will be applied in the coming year to the metal matrix composites studied in this program. Both active techniques noted above will be utilized where appropriate.

2.7 Stress Wave Factor

In a series of recent reports and presented papers, Vary and others [2-6] have discussed the development of a new ultrasonic technique that yields a quantitative parameter that appears to correlate well with some mechanical properties of composite materials. This technique simulates acoustic emission signals in a material by generating high frequency (megahertz) stress waves via a standard ultrasonic pulse generator. The simulated acoustic emissions are counted by standard acoustic emission counting techniques using low frequency (kilohertz) AE transducers. The number of times the received signal crosses the counting threshold in the gated counting time interval is called the stress wave factor. Vary has argued that this number is highly dependent upon the stress wave propagation characteristics of the material. These in turn are highly dependent upon the local material integrity. Utilization of the technique requires the development of careful, standardized experimental techniques. During the past year, initial work has been performed in our laboratory to establish the proper procedures for application of this technique to metal matrix composites. In the coming year, this work will be continued to obtain correlation between the stress wave factor and the ultrasonic attenuation measurement discussed in Section 2.5. Both of these techniques can be set up to measure essentially the same volume of material.

2.8 Mechanical Tests

After the composite specimens have been examined by the various NDT methods, mechanical tests are run to study the effect of defects on mechanical response. The type of mechanical test must be chosen so that the measured response of the material is sensitive to the defect being studied. This is best done by matching the local state of stress to the type of defect. One of the apparent types of defects detected by the nondestructive tests was the interlaminar defect which will be described in the Results section of this report. This type of defect in laminated composites, when acted upon by interlaminar shear stresses, can result in delamination along ply interfaces and shear related fractures.

Perhaps the most feasible mechanical test for studying the interaction between interlaminar shear stress and interfacial defects in the present specimens is the three point (center load) bend test. The magnitude of the shear stress is constant along the length coordinate (x) of the beam and varies with the depth coordinate (y) measured from the neutral axis. Although classical Euler-Bernoulli beam theory assumes that the material is isotropic, homogeneous, and obeys Hooke's law for a one dimensional stress state, the classical theory can be used to calculate normal and shear stresses in unidirectional composite beams of homogeneous construction; i.e., beams in which each ply is identical and the ply interfaces can be neglected. For a rectangular beam of depth h, the interlaminar shear stress is given by

$$\tau_{xy} = \frac{VQ}{Ib} \qquad (1)$$

and the bending normal stress is given by

$$\sigma_x = \frac{My}{I} \tag{2}$$

where V = shearing force

$Q = \int_y^{h/2} ybdy$

I = moment of inertia with respect to the neutral axis

b = width of beam at section where τ_{xy} is computed

M = bending moment

If, however, the beam is not of homogeneous construction in the y direction, the above equations are not applicable for the calculation of shear and normal stresses. In this case, equations developed by Pagano [7] and based on the usual beam theory assumptions may be used to calculate the stress components in a beam of N plies (or regions). The normal stress in the i^{th} ply (measured from the neutral axis) can be written as

$$\sigma_x^i = \frac{2E_i\sigma_m y}{E_n h} \tag{3}$$

where σ_m is the normal stress at $y = \pm h/2$ and E_n is the modulus of the top ply ($i = n$). The stress σ_m expressed in terms of the bending moment M is

$$\sigma_m = \frac{3hME_n}{4bA} \tag{4}$$

where $A = \dfrac{1}{\sum_{i=1}^{n} E_i(h_i^3 - h_{i-1}^3)}$. The normal stress in the i^{th} ply can now be written as

$$\sigma_x^i = \frac{3ME_i y}{2bA} \tag{5}$$

The interlaminar shear stress at the bottom of the r^{th} ply is expressed as

$$\tau_{xy}^{r} = \sum_{i=r}^{n} \int_{h_{i-1}}^{h_i} \frac{d\sigma_x^i}{dx}\, dy \ . \qquad (6)$$

Using equation 5 and the relation $V = \frac{dM}{dx}$ in equation 6 gives

$$\tau_{xy}^{r} = \frac{3V}{4bA} \sum_{i=r}^{n} E_i \left(h_i^2 - h_{i-1}^2\right) \qquad (7)$$

For beams of homogeneous construction, equations 5 and 7 reduce to the classical beam equations for bending and transverse shear stress respectively.

Equations 5 and 7 show that the bending and shear stresses in a nonhomogeneous beam are dependent on the properties of the constituent materials. The magnitude and distribution of these stresses are sensitive to the elastic modulus and thickness of individual plies or regions in the beam. In the present investigation, the regions are defined as the plies of unidirectional Al/Fp composite material and possible interfacial zones of finite thickness made up of matrix rich material. The Al/Fp and interfacial regions produce a material with nonuniform distributions of flexure and interlaminar shear strengths. In many cases, the interfaces are sites of interlaminar failure when acted upon by interlaminar shear stress such as that given by equation 7.

In an earlier investigation, the authors studied the interaction between interlaminar shear stress and interfacial defects in unidirectional graphite polyimide composite laminates [1,8]. Interlaminar shear failures occurred only in those short beam shear specimens which were of

poor quality as determined by ultrasonic C-scan and attenuation measurements. Specimens having less severe initial defects did not fail in a shear mode. Data were analyzed by considering the distribution of the failure loads and noting the failure modes. Those specimens which failed in shear had defective ply interfaces and had failure strengths on the low end of the distribution. The ultrasonic attenutation values correlated with the failure loads and could be used to quantify the defective regions of the material. Stiffness could also be used to indicate the quality of the material.

A three point bend test fixture has been designed, fabricated, and installed on an MTS load frame (Fig. 3). The Al/Fp specimens are presently being instrumented for mechanical testing in both monotonic and cyclic bending. Stiffness, acoustic emission, and ultrasonic attenuation data will be recorded to monitor changes in these parameters throughout the loading history. Real time video thermography, which has proven to be a valuable NDI method to detect and monitor damage growth in boron epoxy, boron aluminum, and graphite epoxy, will be employed to assist in determining the initiation and growth of damage in Al/Fp composites. Also, the specimens will be removed from the test fixure at selected load or cyclic intervals and subjected to C-scan and radiographic inspection. Data obtained during the bend tests will be examined and compared to pre-test NDI data to assess the criticality of initial defects and defects induced by mechanical loads on the failure of the material.

Other loading modes, such as compression, may also be sensitive to initial defects in the specimens. Interfacial regions of matrix rich material will decrease the effective stiffness of the specimen and lower

the value of applied load required to buckle the specimen. Static and cyclic compression tests are planned to further investigate the effect of defects on the response of Al/Fp and Al/W composites.

3.0 Results and Discussion

3.1 Results from C-Scan

Some typical results for ultrasonic C-scans obtained for eight of the flat Al/Fp specimens (Specimen Nos. 6-13) are given in Figures 4-9. The scan marked "test" at the right-hand side of each Figure (a) is the standard specimen discussed in Section 2.2. The gain controls were set each time so that the maximum amplitude of the first echo returning from the reflection plate through the large hole at the top of the standard corresponded to a height of eight divisions on the CRT display. (As noted earlier, this is an arbitrary choice.) The trigger level was then varied as noted in the figure captions, ranging from 4 divisions for Fig. 4 to 7 divisions for Fig. 9. Hence, Fig. 4 has a preponderance of black area indicating that the amplitude of the ultrasonic pulse transmitted through much of the specimen was 50% of that transmitted through the standard. On the other hand, Fig. 7 has a preponderance of white area indicating that the amplitudes of the returning echos were less than 87.5% of that transmitted through the hole in the standard.

One of the first comments to be made concerning the interpretation of the C-scan is the combined effect of the finite beam width and scattering of the beam along the specimen edges. These effects combine to cause an apparent widening of the specimen along with white regions parallel to the edge that appear to be regions of inferior ability for the transmission of the ultrasound. Close observation of the CRT has shown in each case that the white areas along the edges are artifacts caused by the beam-specimen geometry. More precisely, one cannot use the C-scan to locate damaged or flawed regions within approximately 1 mm of the edge. This dimension varies slightly with the trigger lever

settings.

A second, major observation is that of longitudinal striations that appear to some degree in every specimen. The C-scans indicate regions of good and poor ultrasonic transmission across the width of the specimen. While these regions meander along the length of the specimen, sometimes merging and sometimes diverging, they appear to the eye to be distinct layers either related to the original laminae that were used in laying up the plate from which the specimens were cut or indications of flow paths followed by the molten aluminum as it impregnated the mold during the fabrication process. It should be pointed out that the specimens used here were obtained by slicing a 152.4 x 152.4 x 12.7 mm (6 x 6 x 1/2 in) plate across the 12.7 mm thickness. Hence each specimen is oriented such that the width of the specimen is the thickness of the original plate and the laminae in the original plate are perpendicular to the specimen width. In those regions where layering is most distinct in the C-scans, five regions with relatively good ultrasonic transmission properties are found to separate six regions having relatively poor properties. No attempt has been made at this point to obtain further information on the fabrication process. It is presently felt to be desirable to continue work on these specimens to determine, if possible, what these regions are and if the same number can be distinguished by other NDT methods. Too much information concerning the fabrication procedures may force unwarranted conclusions or speculations on data obtained from the NDT tests. This data will be researched and discussed in summary at the conclusion of this work.

Some optical microscopy has been performed on several specimens

that appear to have the most distinctive longitudinal striations in the C-scans. The regions that have the better ultrasonic transmission properties appear to be regions having the densest packing of fibers. Typical micrographs are shown in Fig. 10. Figure 10(a) is a picture of a typical region in the end of the specimen showing a relatively uniform distribution of fibers. Figure 10(b) shows a region of nearly pure matrix extending across the thickness of the specimen. Just below this region is an area of very dense fiber packing. Additional work is being performed to see if a correlation exists between the number of such regions across the specimen thickness and the number of striations in the C-scans.

As noted in Section 2.8 on mechanical tests, some three-point bend tests will be performed on the Al/Fp specimens to determine if these longitudinal regions have any effect on the mechanical properties. It is believed that variations in mechanical properties across the width will evidence themselves most easily by observing any differences in shear across these regions.

A third observation that can be made from the C-scans is that there are some major differences between each specimen. This is perhaps most evident in Figures 7 and 8 which show that specimen No. 7 is a much better transmitter of ultrasound than specimens No. 6 and 8. This observation will be used with later mechanical tests to determine if any interesting or useful correlations exist.

3.2 Results of X-Ray Radiography

The most interesting result obtained in the limited time the material and machine was available to us occurred during tests of the Al/FP specimens. The radiographs of the plate specimens showed linear detail, lines of contrast that run parallel to the length of the specimens. These lines can be discerned in some of the specimens in the radiographs reproduced in Figs. 11 and 12. Although it is difficult to be sure, it appears that the number of lines across the specimen width is the same as that observed in the ultrasonic C-scan patterns. It should be remembered that the width of the specimens is really the thickness of the plate from which they were cut raising the possible interpretation of the lines as the vestiges of the layers of "prepreg" that were stacked up to make the original panel. In any case it is certainly true that some nonuniformity is shown by the radiographs. This radiographic detail only shows up at relatively low voltage settings and relatively long exposure times, and is not equally resolved in each of the specimens suggesting that the location of each specimen in the original panel may have an influence on the degree of this nonuniformity, i.e., it may be that the original plate was not uniform in its plane. These conclusions are, of course, preliminary pending further investigation.

The radiographs of the tungsten-aluminum rods shown in Figs. 13 and 14 were difficult to generate because of the geometry of the rods. Methods to correct the differences in transmitted x-ray intensity are being attempted. In Figs. 13 and 14 the "cone" shaped images are due to geometric effects rather than internal detail. However, some detail is resolved near the edges of the rods. The arrows indicate examples of

such an image. The nature of this detail is, as yet, undetermined. The density of this material makes it difficult to penetrate requiring high voltages and long exposures, not a combination conducive to good radiographic detail. Scattering is a problem that will have to be dealt with. However, tungsten is extremely opaque to x-rays so that, if the geometric and scattering problems can be solved, it should be possible to resolve the filaments easily.

3.3 Eddy Current

The eddy current results to-date have been uninteresting. Scanning with the probe across the width and along the length has shown essentially no variation in the reactance (X) and resistance (R) values measured by the technique. Typical results are given for two specimens in Tables I and II. It is not clear at this point whether the limitations of this technique are due to the nature of the material or to the choice of the particular frequency and probe geometry used.

Table I: Reactance (X) and Resistance (R) Measured across Surface of Al/Fp Specimen by Eddy Current Technique

X–	516	518	518	518	520	528
R–	624	622	624	621	623	620
	516	518	517	518	519	526
	624	622	623	621	623	622
	516	518	516	518	519	528
	623	622	623	623	623	621
	517	518	518	518	520	528
	624	623	624	622	624	622
	518	518	518	518	520	527
	623	623	624	622	624	622
	518	518	518	518	520	529
	624	623	623	622	624	621
	518	518	518	519	520	528
	624	624	623	622	624	623
	519	519	519	519	520	528
	624	624	624	621	624	622
	520	518	519	520	521	528
	624	624	622	621	622	623
	520	519	518	520	521	528
	624	623	623	622	623	622
	521	519	520	520	522	528
	624	623	623	621	622	622
	523	520	520	521	522	529
	624	623	623	621	623	622
	524	520	521	522	522	528
	624	623	623	620	623	622
	525	521	521	522	523	529
	623	622	622	621	623	621
	526	521	522	524	524	529
	622	623	622	622	623	622
	528	522	522	522	523	530
	620	623	620	620	622	622
	532	522	522	524	524	532
	618	622	621	621	622	619

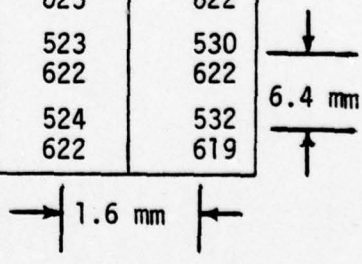

Table II: Reactance (X) and Resistance (R) Measured Across Width of Al/Fp Specimen

DISTANCE	X	R
0	558	548
1 mm	554	550
2	552	551
3	552	552
4	552	551
5	551	551
6	552	551
7	552	551
8	553	550
9	554	549
10	555	548
11	556	546
12	558	543
13	559	540

4.0 Conclusion

At this point in time it is premature to draw any definitive conclusions from the preliminary tests that have been run. The ultrasonic C-scan and the X-ray radiography techniques do, however, indicate that the Al/Fp specimens contain longitudinal patterns. These specimens were cut from a panel that was fabricated by laying up several sheets of Fp prepreg tape in a mold, evacuating the binder from the tape, and introducing molten aluminum into the mold from one end. It appears from the NDE data that this fabrication procedure results in longitudinal layering. The effect of this layering upon the mechanical properties of the material will be studied during the next term of the contract.

In addition, during the coming year, additional NDE data will be obtained on these specimens in an attempt to provide more quantitative information to compare one specimen with another. In particular, the ultrasonic attenuation technique, the stress wave factor technique, and the video-thermography technique will be studied.

References

1. Hayford, D. T., Henneke, E. G., and Stinchcomb, W. W., "The Correlation of Ultrasonic Attenuation and Shear Strength in Graphite-Polyimide Composites", J. of Comp. Materials II, pp. 429-444 (1977).

2. Vary, A. and Bowles, K. J., "Ultrasonic Evaluation of the Strength of Unidirectional Graphite-Polyimide Composites", NASA Technical Memorandum, NASA TMX-73646, April 1977.

3. Vary, A., "Correlations Between Ultrasonic and Fracture Toughness Factors in Metallic Materials", NASA Technical Memorandum, NASA TM-73805, June, 1978.

4. Vary, A. and Bowles, K. J., "Use of an Ultrasonic-Acoustic Technique for Nondestructive Evaluation of Fiber Composite Strength", NASA Technical Memorandum, NASA TM-73813, February, 1978.

5. Vary, A. and Lark, R. F., "Correlation of Fiber Composite Tensile Strength with the Ultrasonic Stress Wave Factor", NASA Technical Memorandum NASA TM-78846, April, 1978.

6. Vary, A., "Quantitative Ultrasonic Evaluation of Mechanical Properties of Engineering Materials", NASA Technical Memorandum, NASA TM-78905, June, 1978.

7. Pagano, N. J., "Analysis of the Flexure Test of Bidirectional Composites", Journal of Composite Materials, Vol. 1, 1967.

8. Stinchcomb, W. W., Henneke, E. G., and Price, H. L., "Use of the Short Beam Shear Test for Quality Control of Graphite-Polyimide Laminates", ASTM STP 626, 1977.

LIST OF FIGURES

LIST OF FIGURES
(continued)

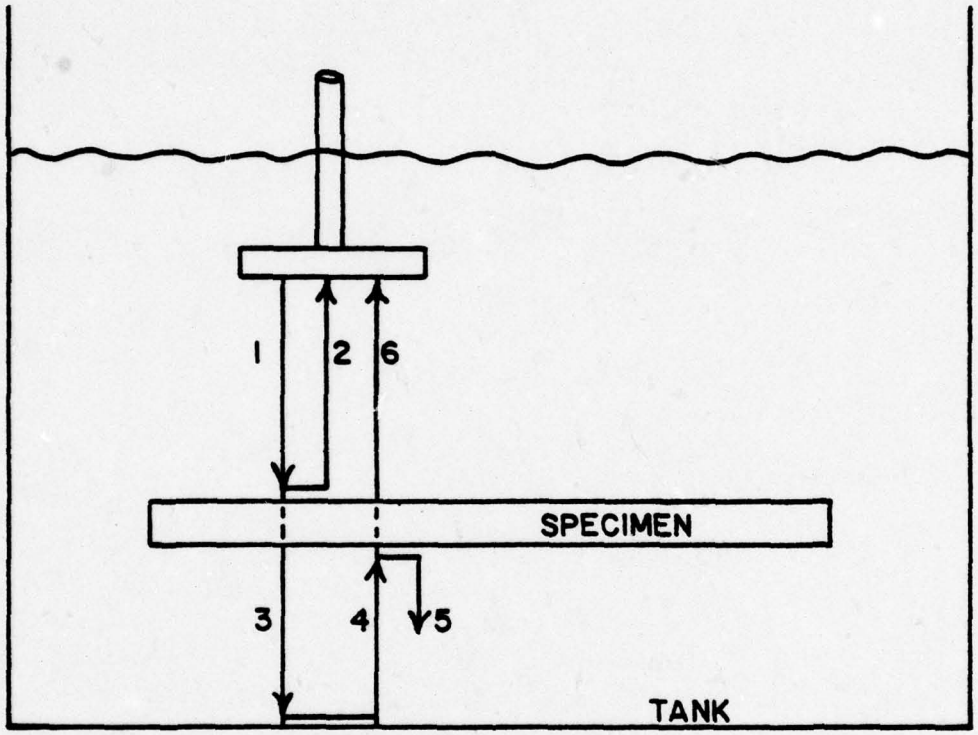

Figure 1 Schematic Representation of Ultrasonic C-scan Test and Echoes

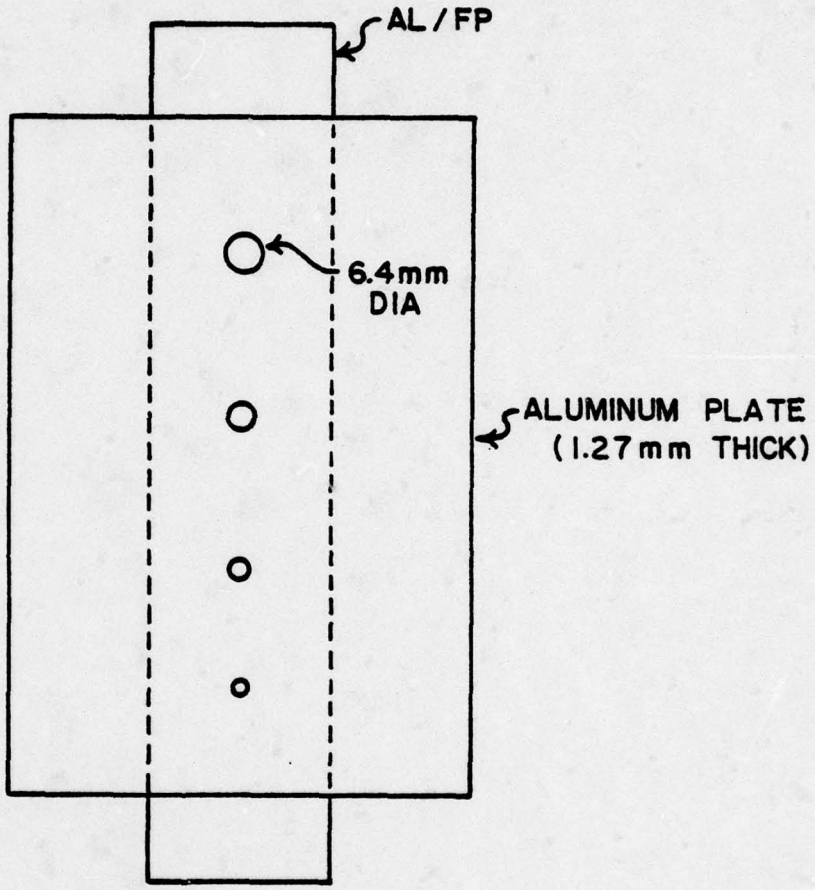

Figure 2 Schematic Representation of Ultrasonic Calibration Specimen

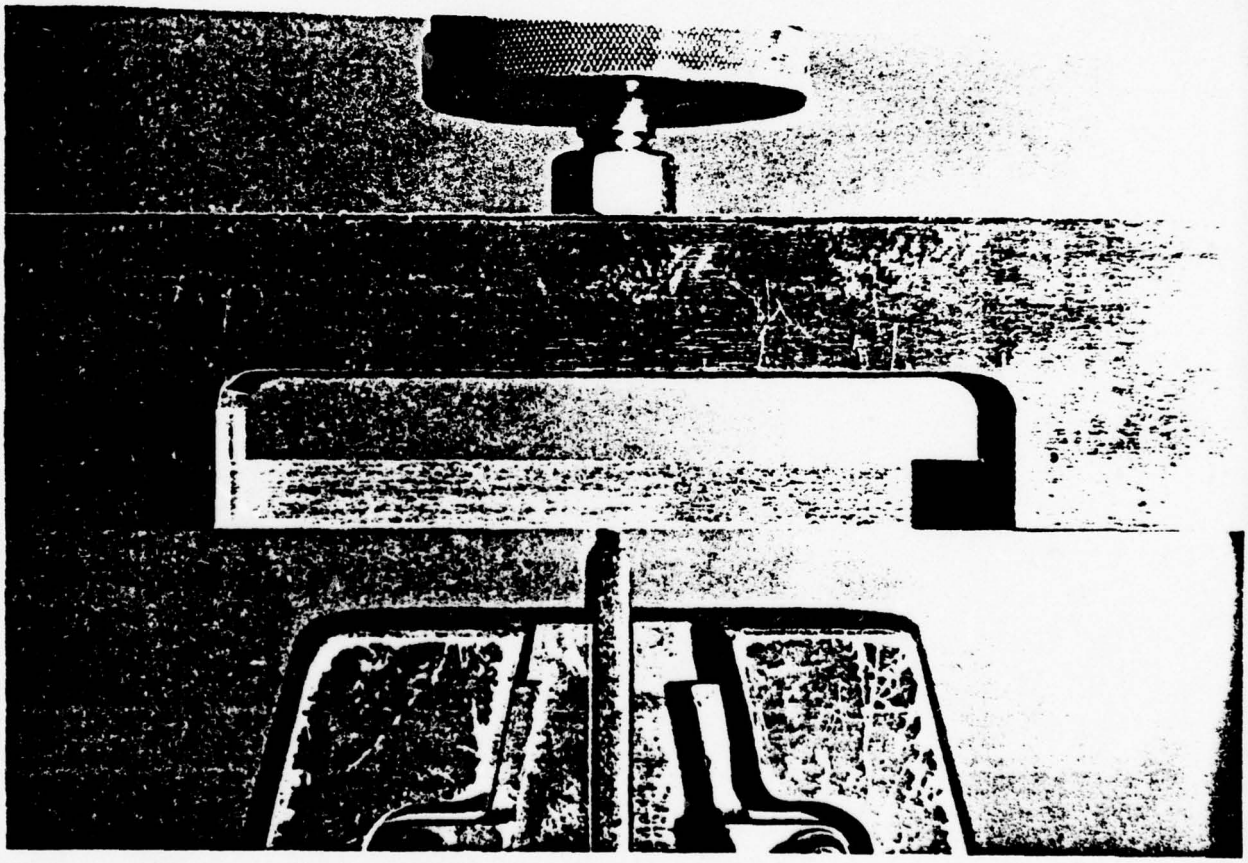

Figure 3 Bend test fixture for static and cyclic loading of Al/Fp Specimens

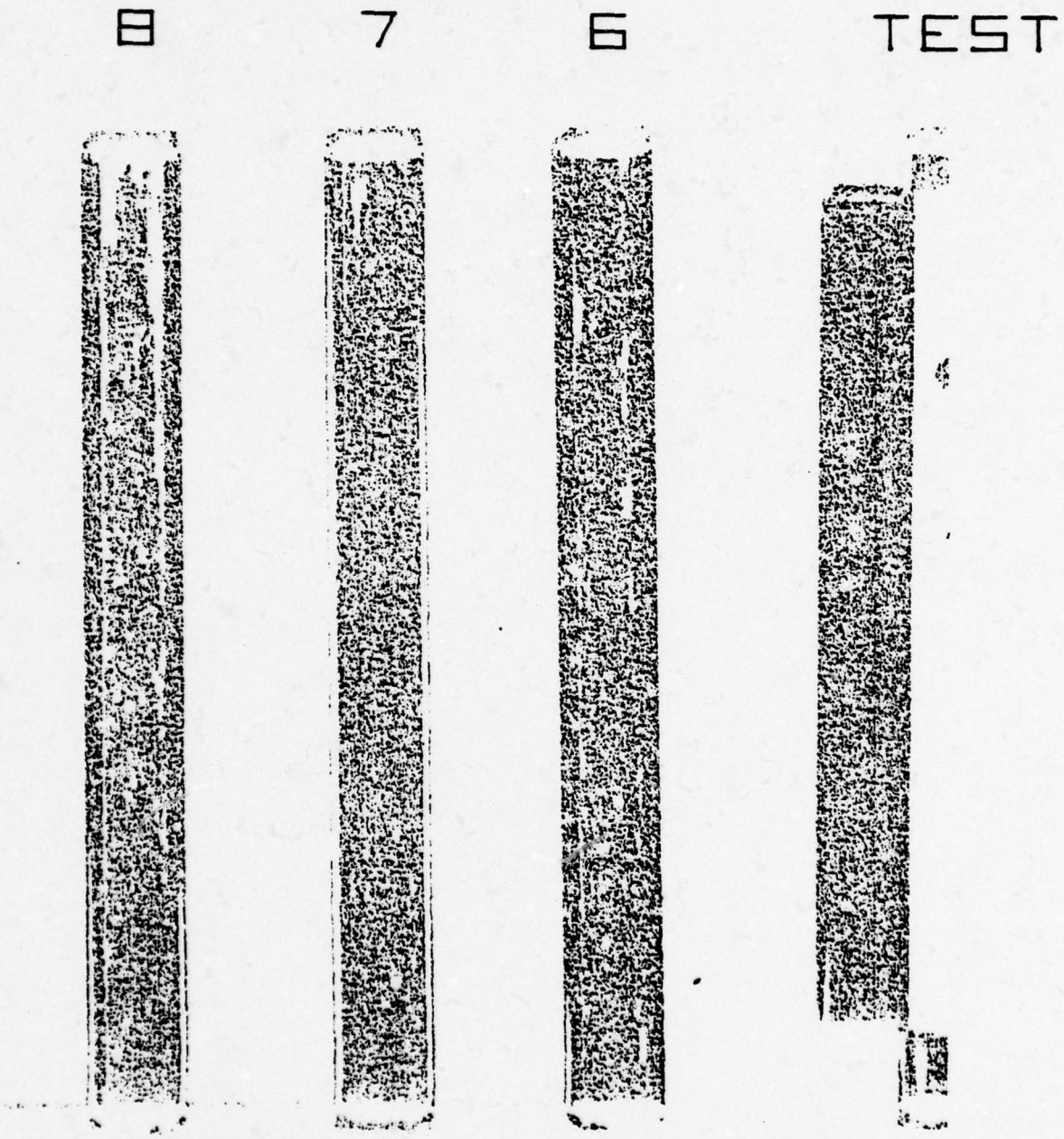

Figure 4(a). C-scan of Al/Fp specimens No. 6-8 and standard. Trigger level set at four divisions.

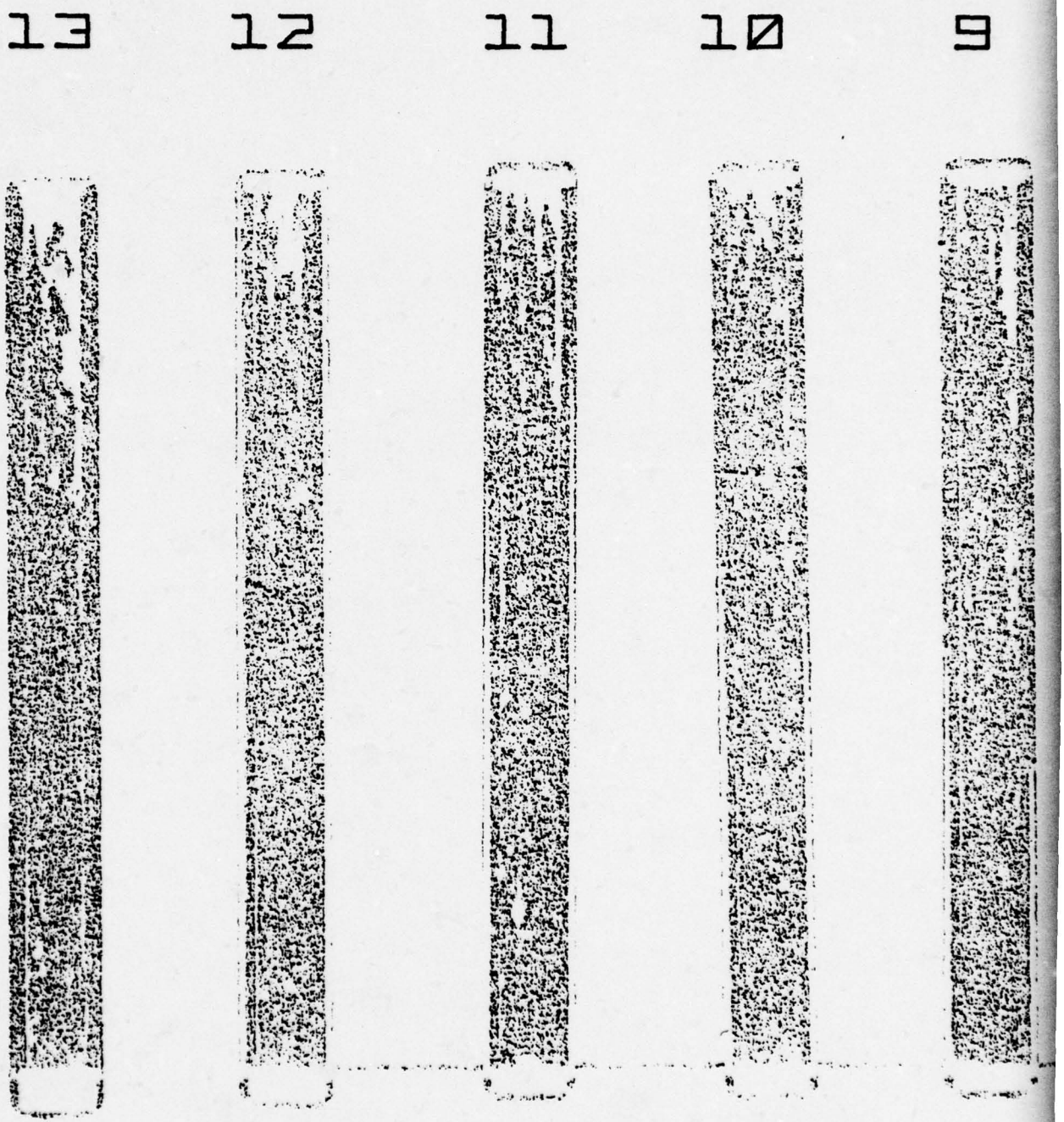

Figure 4(b). C-scan of Al/Fp specimens No. 9-13. Trigger level set at four divisions.

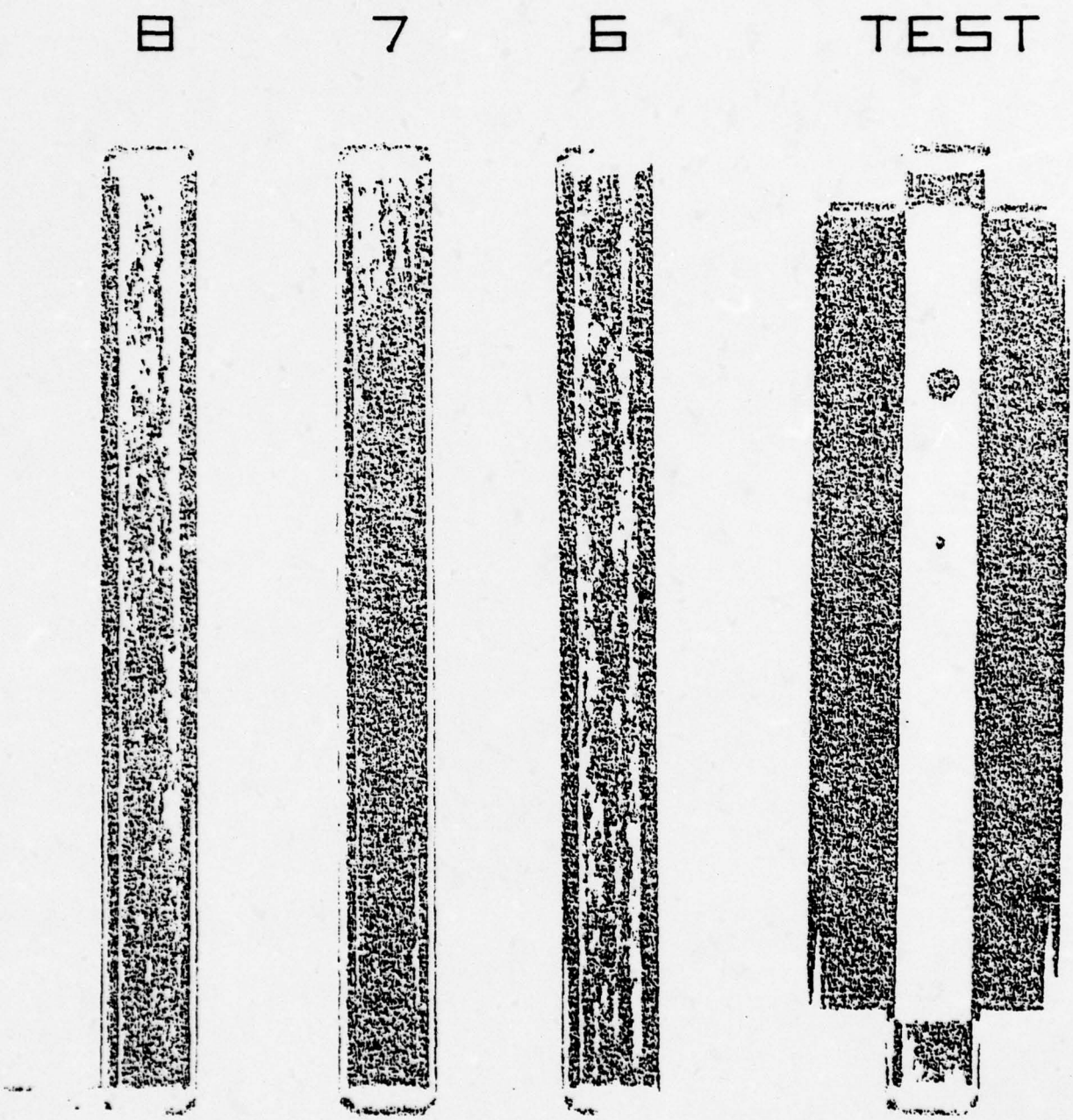

Figure 5(a). C-scan of Al/Fp specimens No. 6-8 and standard. Trigger level set at five divisions.

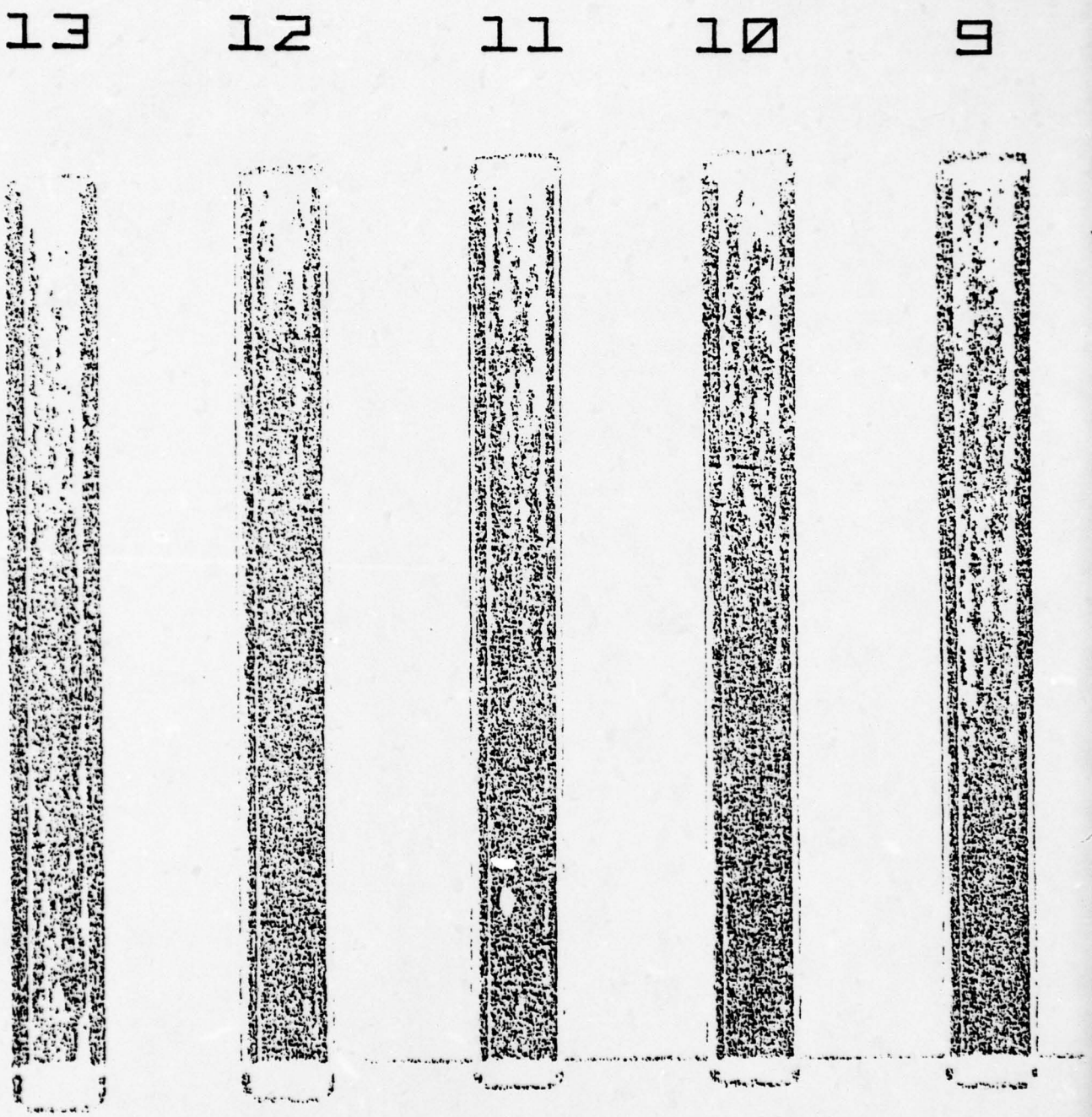

Figure 5(b). C-scan of Al/Fp specimens No. 9-13. Trigger level set at five divisions.

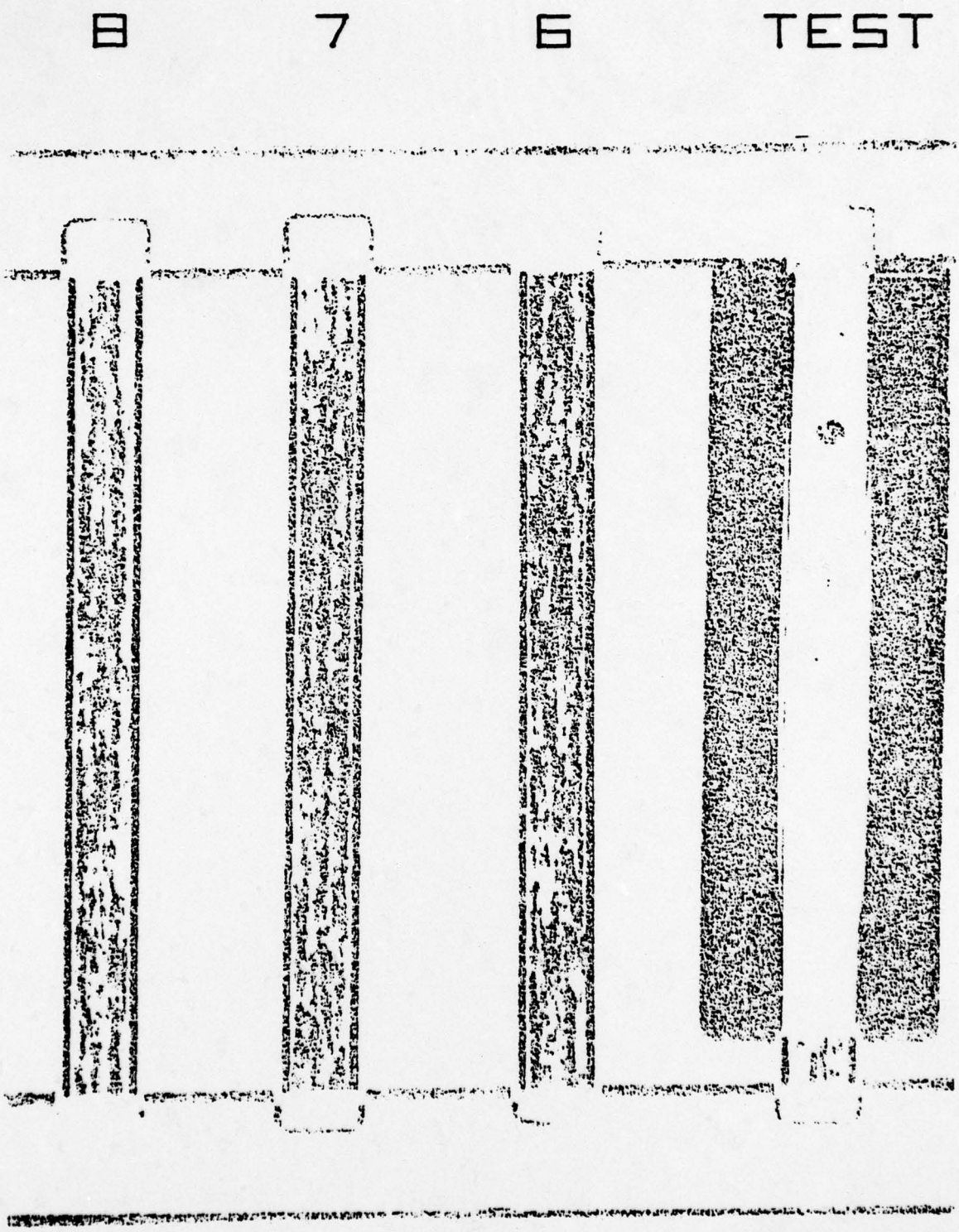

Figure 6(a). C-scan of Al/Fp specimens No. 6-8 and standard. Trigger level set at six divisions.

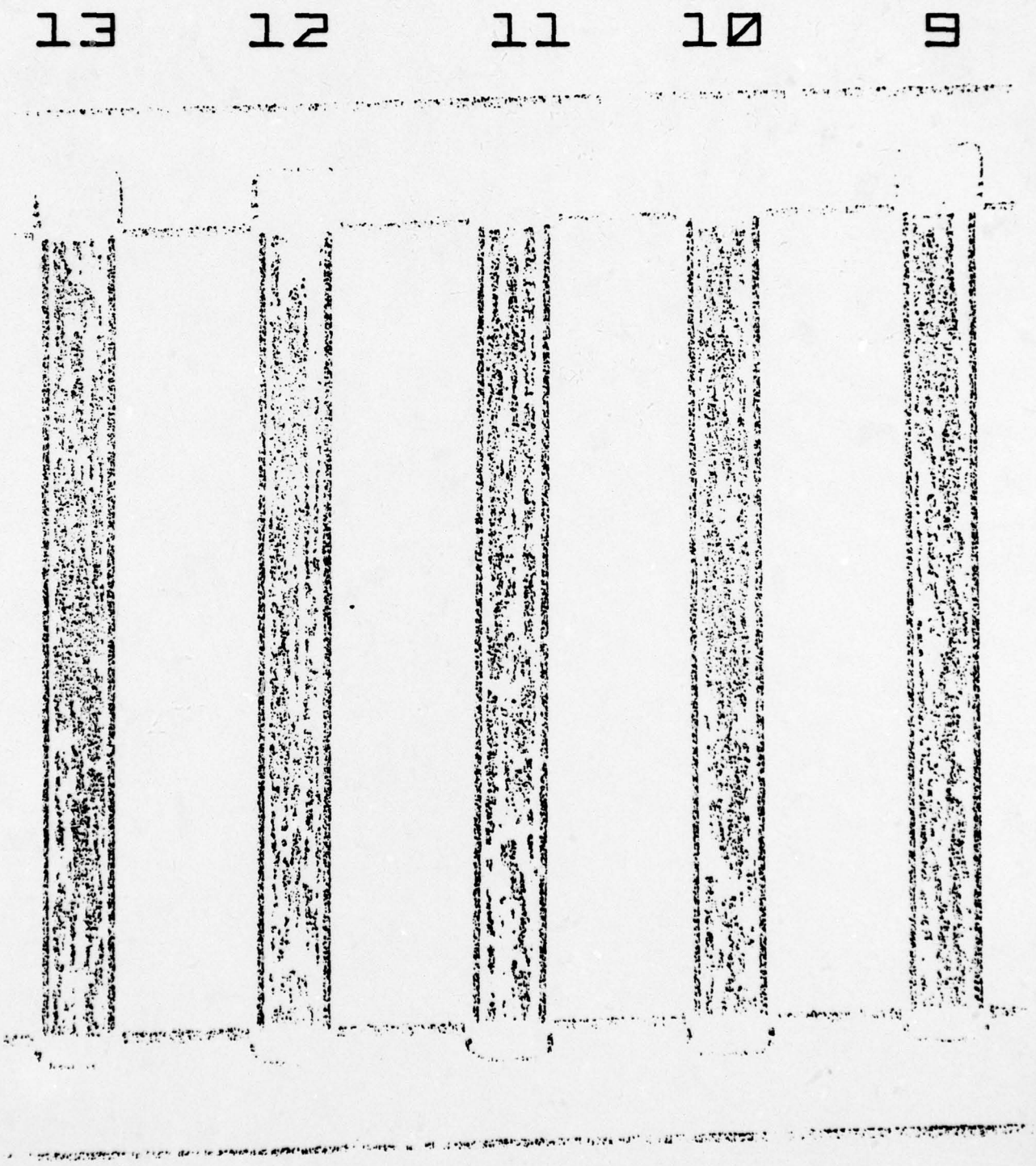

Figure 6(b). C-scan of Al/Fp specimens No. 9-13. Trigger level set at six divisions.

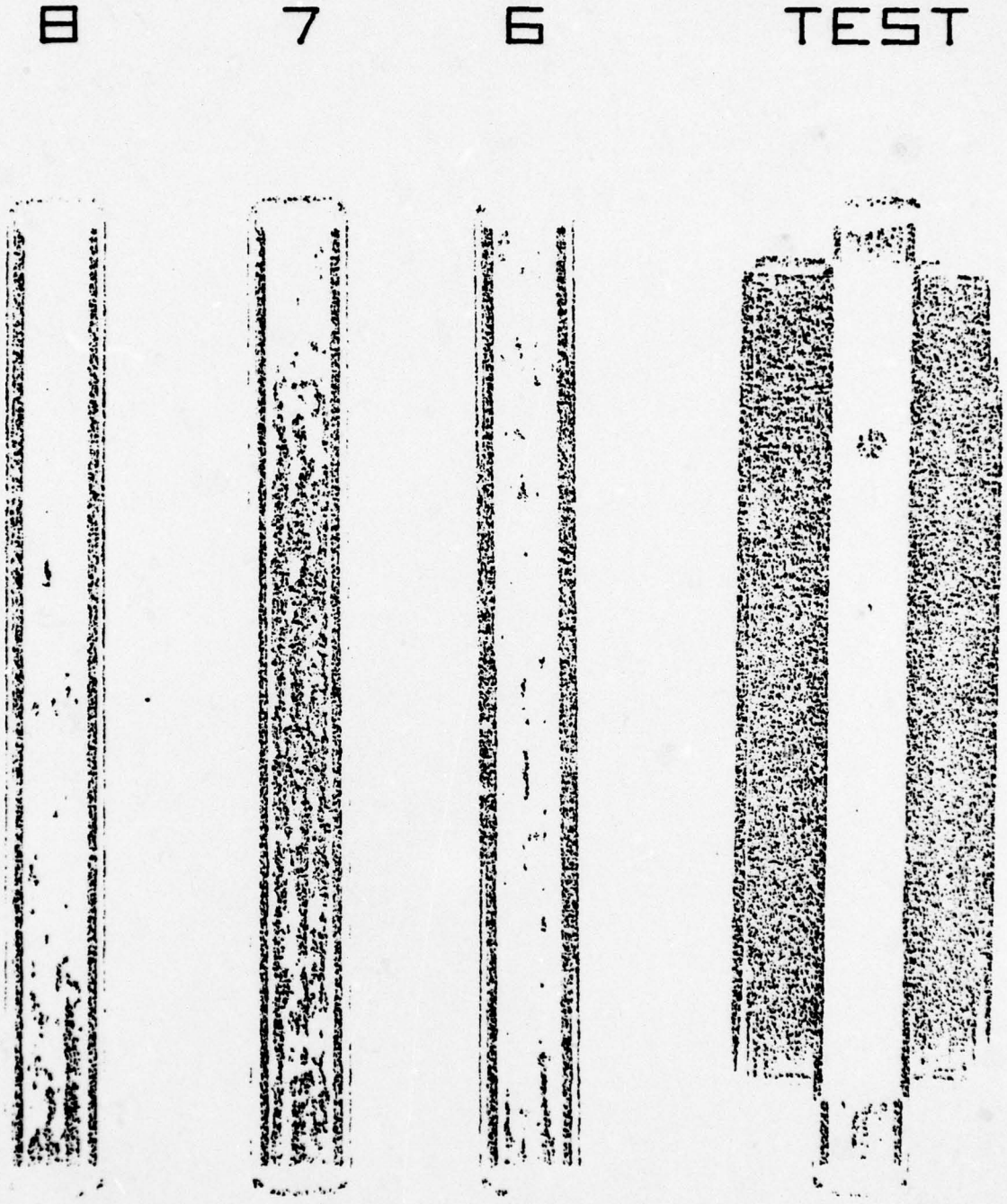

Figure 7(a). C-scan of Al/Fp specimens No. 6-8 and standard. Trigger level set at 6 1/3 divisions.

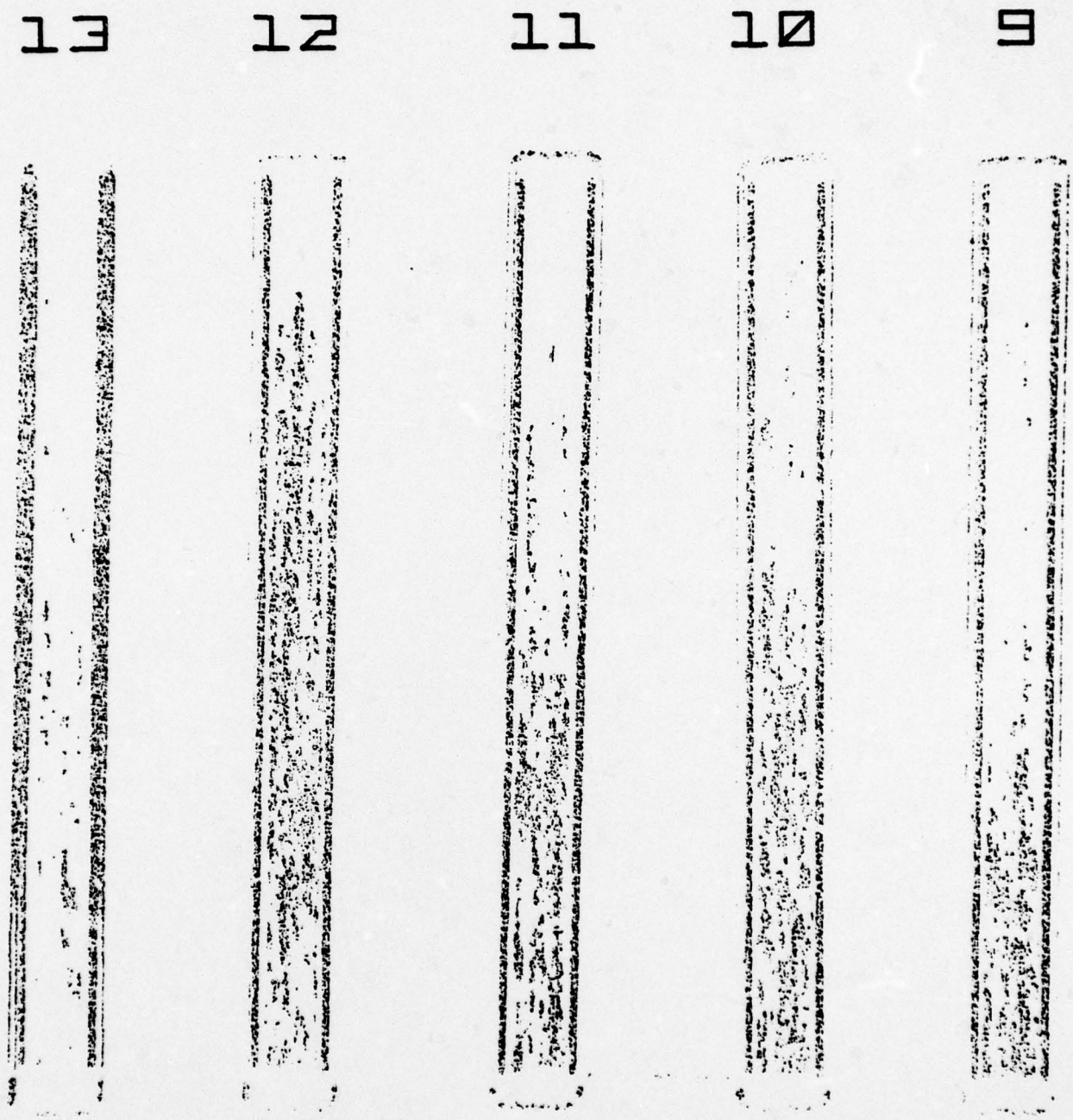

Figure 7(b). C-scan of Al/Fp specimens No. 9-13. Trigger level set at 6 1/3 divisions.

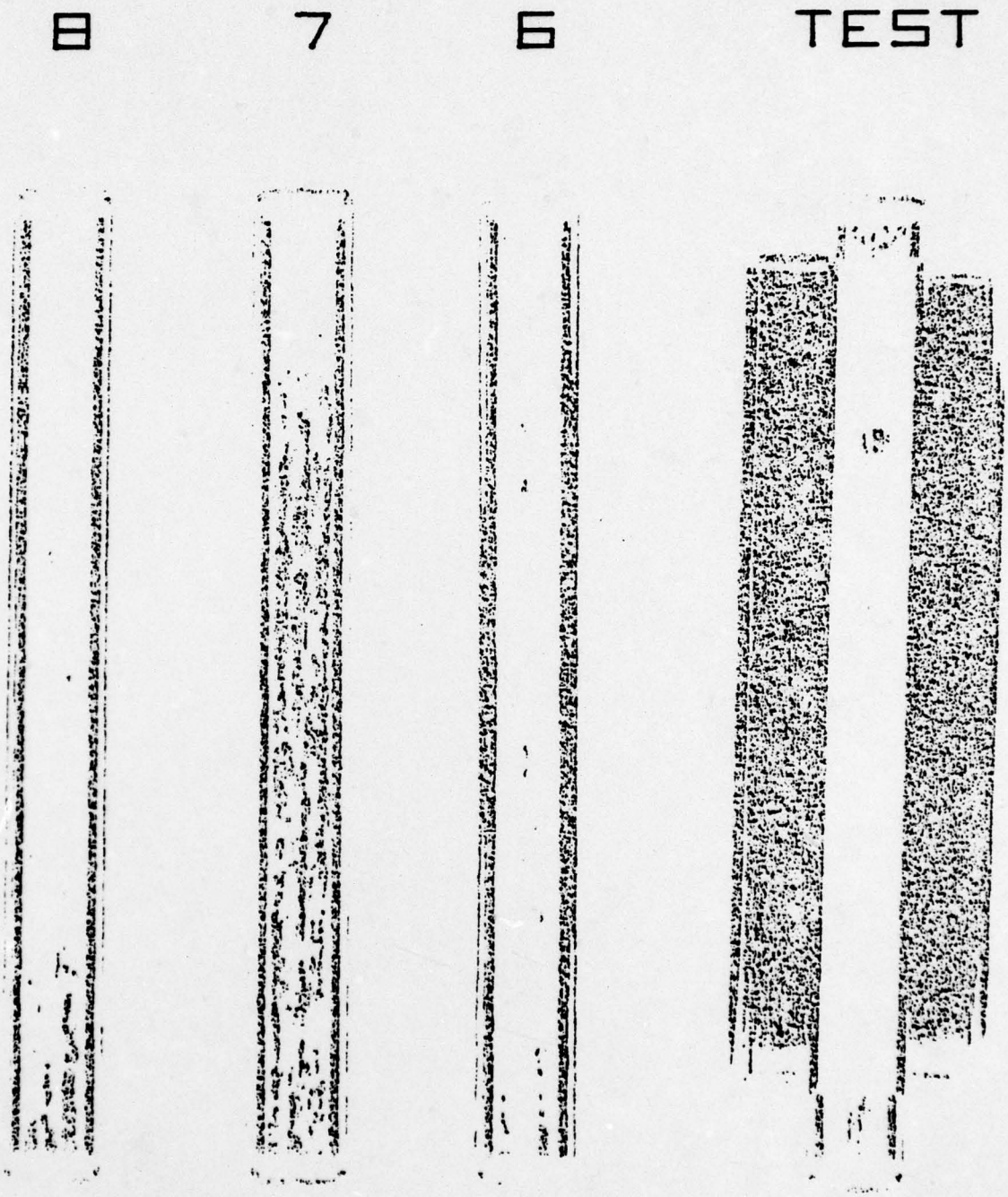

Figure 8(a). C-scan of Al/Fp specimens No. 6-8 and standard. Trigger level set at 6 2/3 divisions.

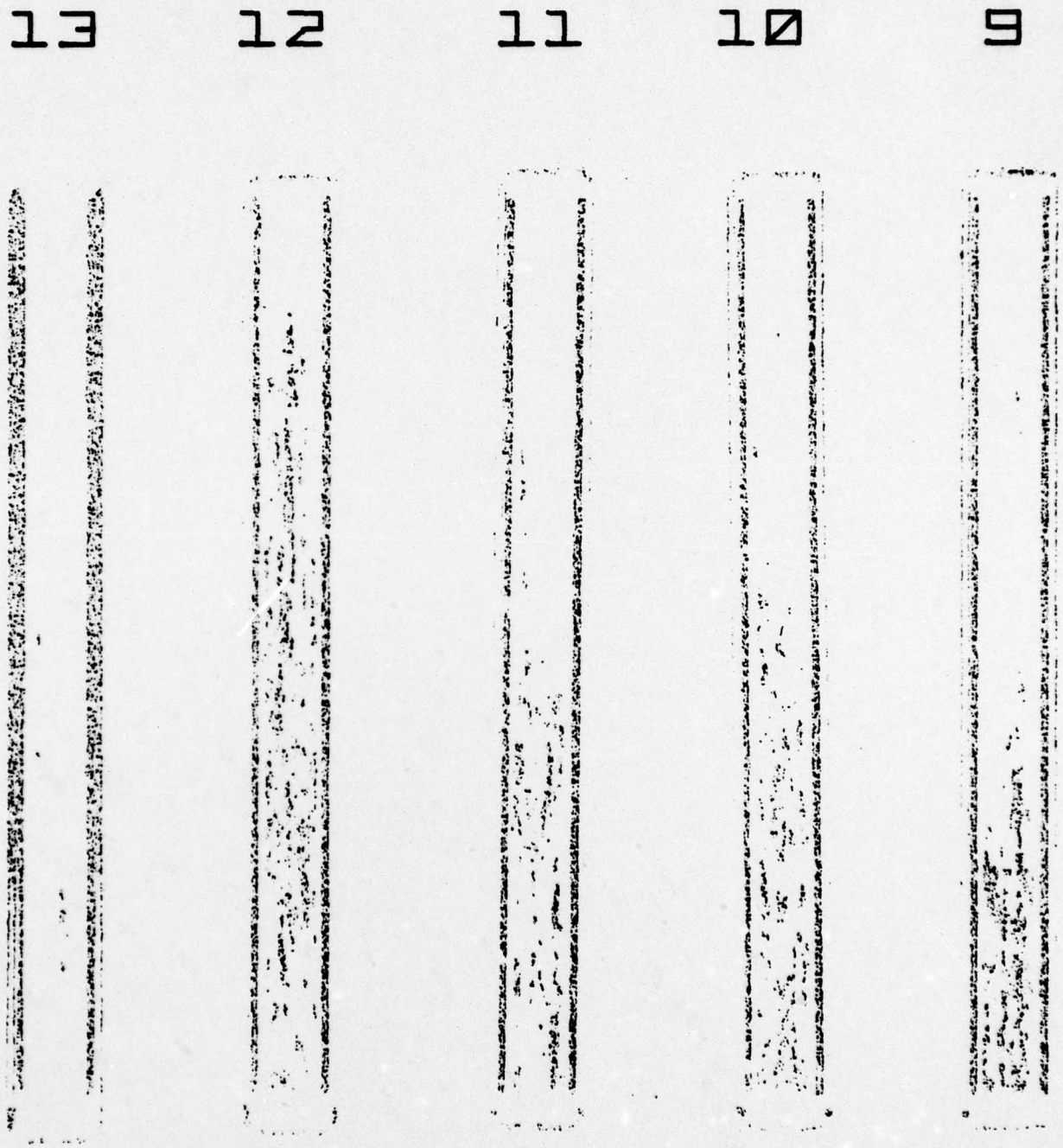

Figure 8(b). C-scan of Al/Fp specimens No. 9-13. Trigger level set at 6 2/3 divisions.

Figure 9(a). C-scan of Al/Fp specimens No. 6-8 and standard. Trigger level set at seven divisions.

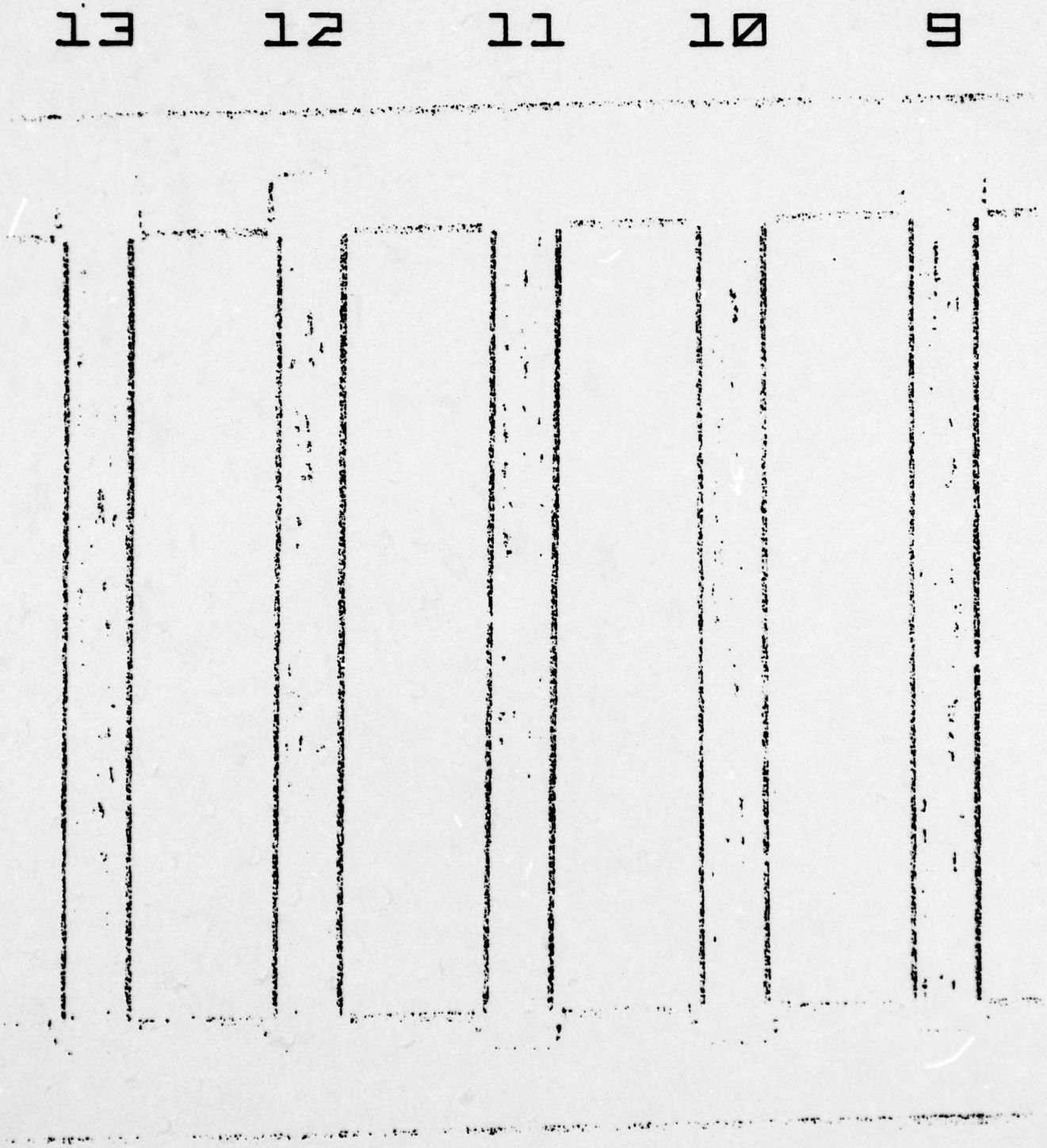

Figure 9(b). C-scan of Al/Fp specimens No. 9-13. Trigger level set at seven divisions.

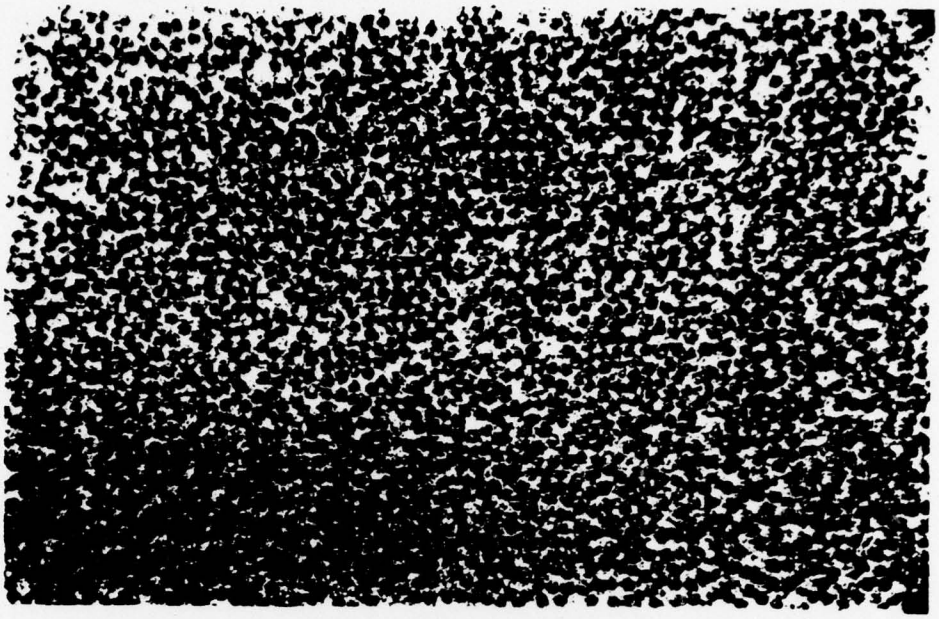

(a)

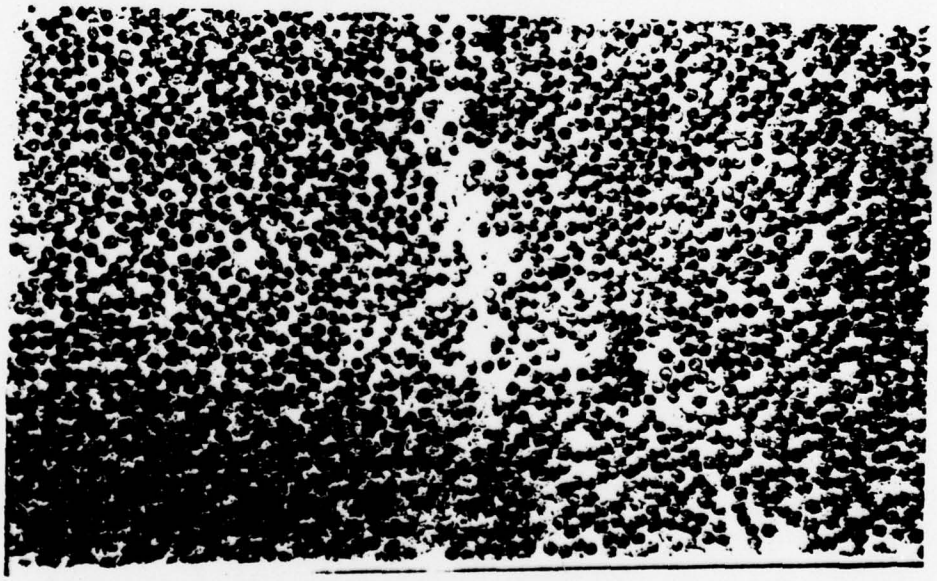

(b)

Figure 10(a). Photomicrograph of typical region in Al/Fp with uniform distribution of fibers.

(b). Photomicrograph of region containing an area with nearly pure matrix and an area dense with fibers.

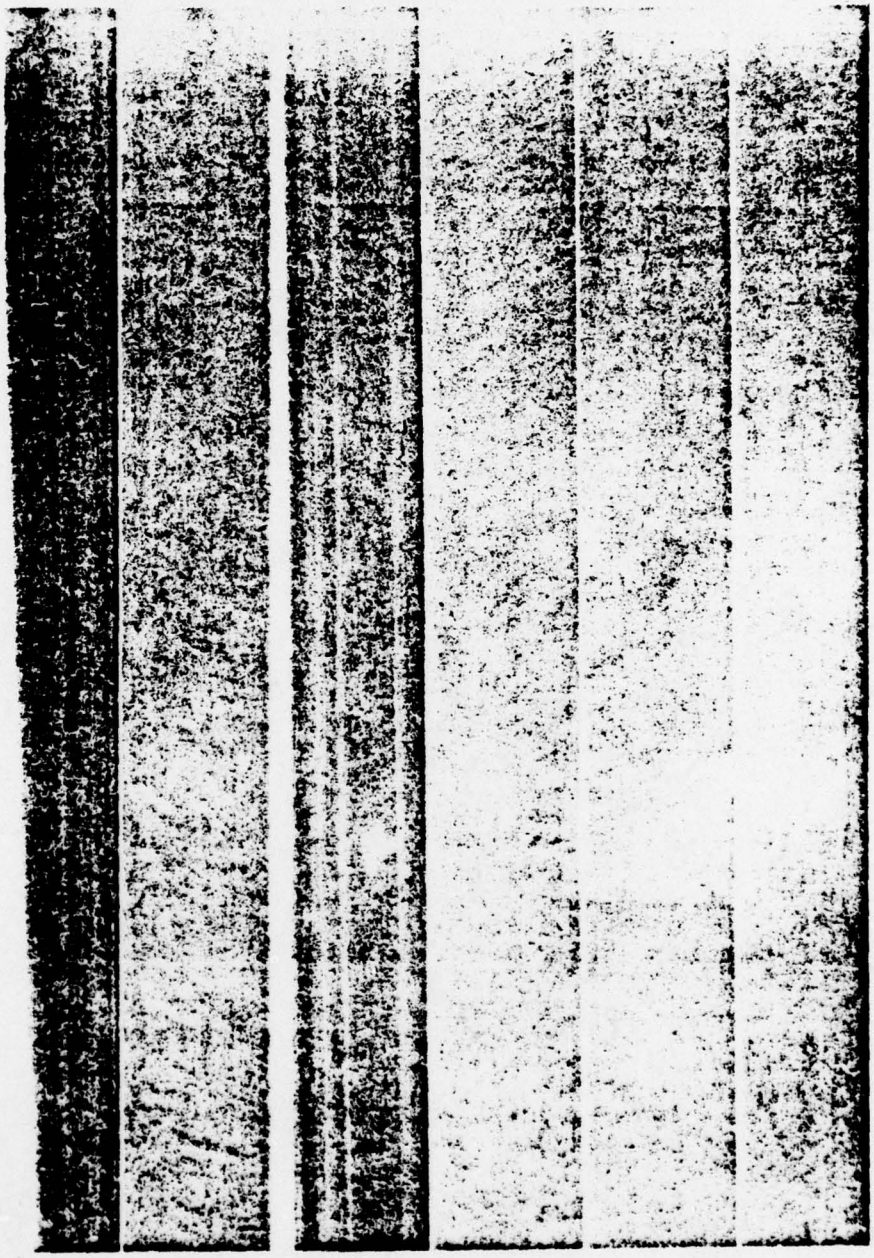

Figure 11. X-Ray radiograph of Al/Fp plate specimens.

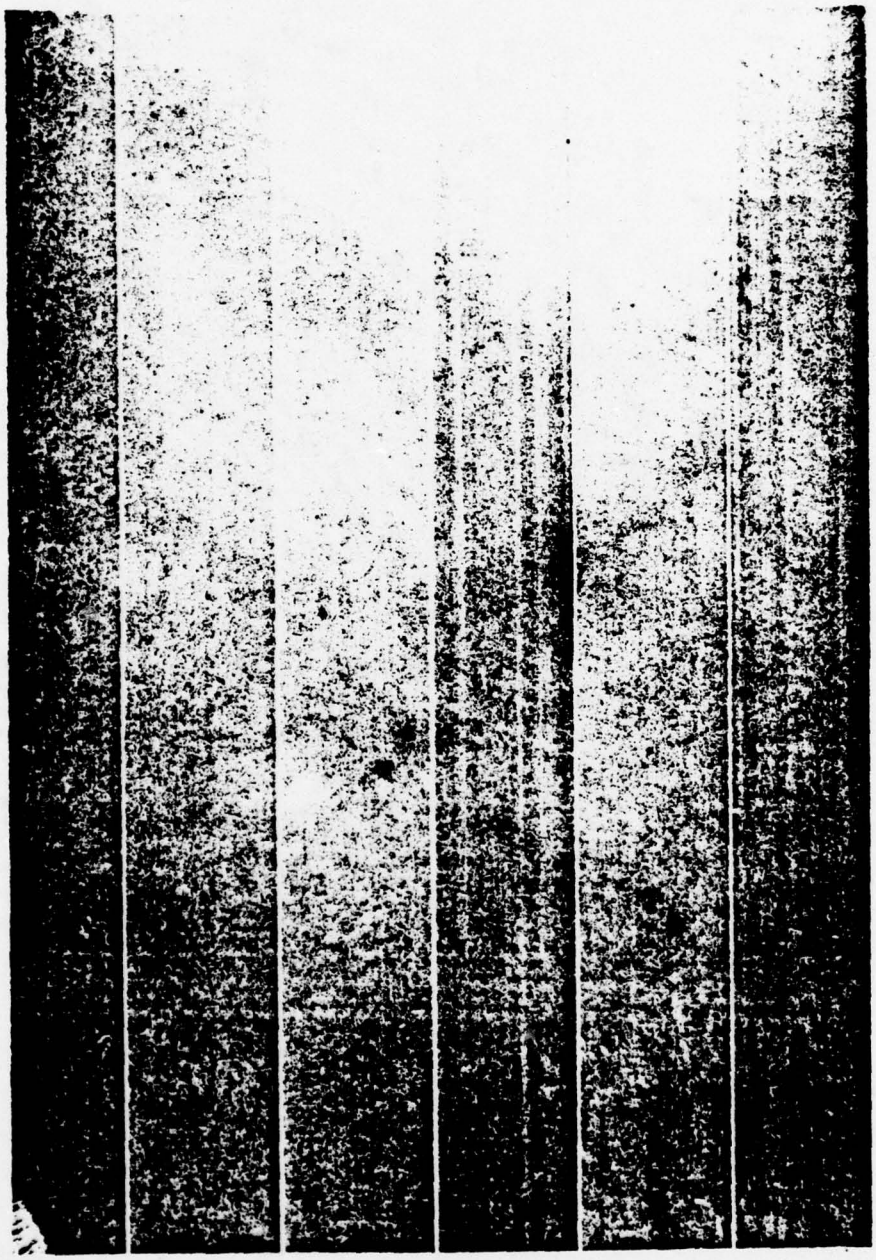

Figure 12. X-Ray radiograph of Al/Fp plate specimens.

Figure 13. X-Ray radiograph of W/Al cylindrical rods. Arrows indicate possible linear detail in specimens.

Figure 14. X-Ray radiograph of W/Al cylindrical rods. Arrows indicate possible linear detail in specimens.